

Probing the Biogeochemical Behavior of Technetium Using a Novel Nuclear Imaging Approach

GAVIN LEAR,^{†,*} JOYCE M. MCBETH,^{†,∇}
CHRISTOPHER BOOTHMAN,[†]
DARREN J. GUNNING,[†] BEVERLY L. ELLIS,[‡]
RICHARD S. LAWSON,[‡]
KATHERINE MORRIS,[§] IAN T. BURKE,[§]
NICHOLAS D. BRYAN,^{||}
ANDREW P. BROWN,[⊥] FRANCIS R. LIVENS,^{||}
AND JONATHAN R. LLOYD^{*,†}

Williamson Centre for Molecular Environmental Science, School of Earth, Atmospheric and Environmental Sciences, The University of Manchester, M13 9PL, U.K., Department of Nuclear Medicine, Manchester Royal Infirmary, Oxford Road, M13 9WL, U.K., School of Earth and Environment, University of Leeds, LS2 9JT, U.K., Centre for Radiochemistry Research, School of Chemistry, The University of Manchester, M13 9PL, U.K., and Institute for Materials Research, University of Leeds, LS2 9JT, U.K.

Received October 20, 2008. Revised manuscript received March 13, 2009. Accepted April 1, 2009.

Dynamic γ -camera imaging of radiotracer technetium (^{99m}Tc) was used to assess the impact of biostimulation of metal-reducing bacteria on technetium mobility at 10^{-12} mol L^{-1} concentrations in sediments. Addition of the electron donor acetate was used to stimulate a redox profile in sediment columns, from oxic to Fe(III)-reducing conditions. When ^{99m}Tc was pumped through the columns, real-time γ -camera imaging combined with geochemical analyses showed technetium was localized in regions containing biogenic Fe(II). In parallel experiments, electron microscopy with energy-dispersive X-ray (EDX) mapping confirmed sediment-bound Tc was associated with iron, while X-ray absorption spectroscopy (XAS) confirmed reduction of Tc(VII) to poorly soluble Tc(IV). Molecular analyses of microbial communities in these experiments supported a direct link between biogenic Fe(II) accumulation and Tc(VII) reductive precipitation, with Fe(III)-reducing bacteria more abundant in technetium immobilization zones. This offers a novel approach to assessing radionuclide mobility at ultratrace concentrations in real-time biogeochemical experiments, and confirms the effectiveness of biostimulation of Fe(III)-reducing bacteria in immobilizing technetium.

* Corresponding author phone: +44 161 275 7155; fax: +44 161 306 9361; e-mail: jon.lloyd@manchester.ac.uk.

[†] Williamson Centre for Molecular Environmental Science, School of Earth, Atmospheric and Environmental Sciences, The University of Manchester.

[‡] Department of Nuclear Medicine, Manchester Royal Infirmary.

[§] School of Earth and Environment, University of Leeds.

^{||} Centre for Radiochemistry Research, School of Chemistry, The University of Manchester.

[⊥] Institute for Materials Research, University of Leeds.

[∇] Present address: School of Biological Sciences, University of Auckland, Auckland 1001, New Zealand.

[∇] Present address: Bigelow Laboratory for Ocean Sciences, West Boothbay Harbor, Maine, 04575.

Introduction

Technetium-99 (^{99}Tc) is a β -emitting product of nuclear fission and a significant contaminant in effluents from nuclear facilities and sediments affected by legacy wastes from nuclear fuel cycle operations (1–5). Technetium has a long half-life of 2.1×10^5 years (^{99}Tc) and high environmental mobility as the pertechnetate anion (Tc(VII); TcO_4^-) which dominates in oxic conditions (4). These factors make the presence of Tc in the environment a matter of ongoing concern. There has been considerable interest in the biogeochemical behavior of technetium in contaminated sediments, as anaerobic bacteria can potentially reduce soluble Tc(VII) to the low-valence, poorly soluble form Tc(IV) (3, 6–10). Tc(IV) is expected to form hydrous TcO_2 -like phases or, at very low concentrations, to sorb as Tc(IV) to mineral phases, effectively immobilizing the radionuclide. Reduction can be achieved enzymatically (11–13) or through indirect mechanisms mediated by Fe(II) and sulfide formed by anaerobic bacteria respiring Fe(III) and sulfate, respectively (3, 6, 8, 11, 14, 15). Stimulation of anaerobic microbial processes through the controlled addition of electron donor into the subsurface offers considerable potential for the sustained remediation of Tc(VII) in situ (16). However, despite the obvious interest in harnessing the potential for metal-reducing bacteria to reduce Tc(VII) in sediments through biostimulation, many of the studies in the literature have been carried out using ^{99}Tc with concentrations typically in the 10^{-6} molar range. Indeed, there is little information on the effectiveness of bioreduction at the very low concentrations of technetium typically observed at contaminated sites (<1 Bq L^{-1} or 10^{-11} to 10^{-12} mol L^{-1}). Here, a noninvasive, sensitive, real-time technique utilizing the isotope ^{99m}Tc has been used to probe the effectiveness of technetium immobilization at ca. 10^{-12} molar concentrations in sediments primed for the reduction of Tc(VII). This will explore the potential for in situ bioremediation strategies at in situ Tc concentrations.

The imaging of 10^{-12} mol L^{-1} Tc is common in medical imaging applications (4, 17) using ^{99m}Tc , an isomer state of ^{99}Tc with a half-life of only 6 h. This short-lived isotope has also been used as a conservative tracer in hydrological and civil engineering experiments (18–22) but has not yet been applied to bioremediation studies. In sediment environments, indigenous anaerobic microbial communities and associated changes in mineralogy and geochemistry potentially have a profound impact on technetium mobility (3, 6–8, 15). The aim of this study was therefore to use γ -camera imaging of ^{99m}Tc migration through biostimulated heterogeneous sediment columns, combined with geochemical, mineralogical, and microbial characterization of the sediments to identify the links between geomicrobiological activity and the mobility of the radionuclide over a range of environmentally relevant concentrations from 10^{-4} to 10^{-12} mol L^{-1} .

Experimental Section

Safety. ^{99}Tc is a radioactive beta-emitter (half-life 2.13×10^5 years; $E_{\text{max}} = 294$ keV) and should be handled in a properly equipped radiochemistry laboratory. The possession and use of radioactive materials is subject to statutory controls.

Microcosm and Sediment Column Construction. Sediments were obtained from the U.S. Department of Energy (DoE) Environmental Remediation Sciences Division (ERSD, formerly NABIR) Field Research Center (FRC) located in Oak Ridge, Tennessee. This extensively studied site is contaminated with a range of organic and inorganic pollutants

including radionuclides derived from the Y-12 plant that were disposed of in waste ponds over a ca. 30 year period (for more details on the site and sampling locations, and a comprehensive list of publications, please refer to <http://www.esd.ornl.gov/orifrc/>). Our study used sediments collected anoxically from below the water table in the background area (uncontaminated and located approximately 4 km from the source area) and in the contaminated Area 2 (located approximately 250 m from the source of the major contaminant plume). The sediments are unconsolidated, clay-rich saprolite, comprising interbedded shale, siltstone, and limestone, with high porosity and low permeability.

Sediment microcosms were prepared anaerobically using 10 g of FRC background area sediment (homogenized from core collected at 3–3.3 m depth in borehole FB610 located near well FW301) and 50 mL of basal freshwater medium (23) in triplicate 100 mL serum bottles. Bottles were amended with 10 mM acetate to stimulate bioreduction and incubated in the dark for 64 days at 20 °C. Triplicate oxic controls were also prepared. In addition, biogenic magnetite microcosms were prepared by adding resting cells of *Geobacter sulfurreducens* to basal freshwater medium containing 50 mM poorly crystalline iron oxide and incubating for 14 days (24, 25).

To visualize the transport of ^{99m}Tc -associated activity through a redox zoned sediment column in real time, columns were constructed under aerobic conditions using sediment from FRC contaminated Area 2 which was homogenized from core material collected at 6.7–7 m depth in borehole FB073 near well FW203. Sediment was slurried 1:1 (w/v) with circumneutral basal freshwater medium and packed into glass columns (length, 9 cm; I/D 1 cm; volume, 7 cm³) blocked at one end with glass wool. The sediment slurry had been amended with 50 mM Na-acetate as an electron donor to stimulate Fe(III)-reduction, and the final saturated porosity was ca. 0.3 mL of water per mL of sediment. Columns were incubated in the dark at room temperature until visual inspection showed development of a gray-green coloration characteristic of biological Fe(III)-reduction in the lower part of the column, indicating the development of a redox gradient (~21 °C, 6 weeks).

γ -Camera Imaging of ^{99m}Tc -Associated Activity. Columns and microcosms were transported to the Manchester Royal Infirmary (UK) for imaging with a GE Millennium Multi-Purpose Rectangular (MPR) field γ -camera (GE Medical Systems, Milwaukee, WI) with a high-resolution collimator (2 mm holes, accuracy of ± 0.5 cm). Sealed microcosms were spiked with 0.1 mL of deionized water containing 10 MBq of ^{99m}Tc activity as pertechnetate (final concentration ca. 10 pM). Columns were injected with 0.5 mL of deionized water containing ca. 25 MBq (spike concentration 2.5 nM) of ^{99m}Tc through a rubber septum in a T-piece opening into the column fluid headspace. Columns were pumped with circumneutral N₂ sparged basal freshwater medium at a flow rate of 7 mL hr⁻¹ to deliver the ^{99m}Tc spike into the column. After injection, gamma camera images of both microcosms and column experiments were taken at 20 min intervals for the first hour and then at hourly intervals until 14.5 h. With a total packed sediment volume of 7 mL, and a saturated porosity of 0.3 mL of water per mL of sediment, 47 pore volumes of basal freshwater medium (100 mL) passed through the column during the experiment. Once imaging was complete, samples were stored at 4 °C for 5 days to allow ^{99m}Tc to decay to background levels. Count data analysis and export of images from γ -camera data acquisition were conducted using Xeleris workstation imaging software (GE Medical Systems, Milwaukee, WI). Count data from vertical sections through the center of each column for hourly time points were decay corrected.

Analysis of Sediment Chemistry and Microbiology. Following γ -camera analysis and ^{99m}Tc decay, columns were

sealed in an oxygen-free environment at –80 °C. When frozen, columns were placed within an argon filled box (oxygen free), and the frozen sediment core was split into horizontal sections of ca. 0.7 cm under argon gas using a band saw. These sediment “discs” were subsequently analyzed for geochemical parameters and molecular (DNA) markers. Weak acid (0.51 HCl) extractable Fe(II) and total Fe(III) concentrations were measured spectrophotometrically in triplicate using the ferrozine assay (Supporting Information Table SI-4 notes; 26, 27).

DNA was extracted from the sediment column at depths of 0.7, 2.1, 3.4, and 9 cm (the bottom of the sediment column) using a PowerSoil DNA Isolation kit (Mo Bio Laboratories, Inc., CA). Nucleic acids were resuspended in sterile, nuclease-free water and stored at –20 °C until analysis. To assess the diversity of the bacterial communities present within sediment zones, a conserved region of the 16S rRNA gene was amplified by PCR. Primers used in this study are summarized in Table SI-3. Initial use of the primers 8F^{forward} (28, 29) and 519R^{reverse} (30) yielded no product utilizing a range of PCR regimes. Consequently, a nested PCR was undertaken using the primers (a) 8F and 1492R (29) and then (b) 530F (31) and 943R (32) as follows: (i) 95 °C for 5 min; (ii) 35 cycles of 95 °C for 30 s, either (a) 57.4 °C or (b) 62.9 °C for 30 s, and then 72 °C for 5 min, (iii) 72 °C for 10 min. PCR was also undertaken to assess the genetic diversity of the Fe(III)-reducing family *Geobacteraceae* using the 16S rRNA gene primers GEO494F (33) and GEO825R (34) as follows: (i) 95 °C for 5 min; (ii) 35 cycles of 95 °C for 30 s, 58 °C for 30 s, 72 °C for 30 s, and then (iii) 72 °C for 3 min. The presence of amplification products was verified by electrophoresis in 1% agarose gels, stained with ethidium bromide. PCR products were purified using a QIAquick Purification kit (Qiagen Ltd., Crawley, UK) and cloned into a pCR2.1 vector, using a TA Cloning kit (Invitrogen Ltd., Paisley, UK) and competent *Escherichia coli* cells (One Shot TOP10, Invitrogen Ltd.), according to manufacturers instructions. Approximately 30 recombinant clones were selected by ampicillin resistance and blue/white colony screening before the presence of the 16S rRNA gene fragment was verified by PCR and agarose gel electrophoresis. Clones were separated into Operational-Taxonomic-Units (OTUs) based upon the similarity of Restriction-Fragment-Length-Polymorphism (RFLP) profiles prepared using the restriction endonucleases *Sau3A1* and *Msp1*, and sequenced as described previously (6, 7). Sequences were analyzed against the NCBI (USA) nucleotide-nucleotide BLAST database (<http://www.ncbi.nlm.nih.gov>) and matched to known 16S rRNA sequences (35). Sequences have been submitted to the NCBI GenBank database (accession numbers EF113250–EF113299, Tables SI-1 and SI-2).

To assess changes in the numbers of Fe(III)-reducing bacteria affiliated with the family *Geobacteraceae*, qPCR was undertaken using appropriate primers (GEO494F (33) and GEO825R (34)). A standard curve for the qPCR reaction was created by plotting the cycle threshold values of the qPCR performed on a dilution series of DNA obtained from *Geobacter sulfurreducens* (GenBank Accession Number U13928) against the log of DNA template concentration. Dilution series concentrations ranging from 2 ng μL^{-1} to 0.2 pg μL^{-1} , were analyzed in triplicate and had an R² value of 0.87. PCR amplification was performed in triplicate on a Stratagene MX3000P qPCR machine using 0.15 μM of each primer and qPCR SYBR Green Master Mix (Stratagene) with an initial step of 94 °C for 10 min followed by 40 cycles of 94 °C for 30 s, 58 °C for 30 s, and 72 °C for 30 s. A dissociation curve was run between 94 and 58 °C to check primer specificity. Cycle threshold was determined automatically.

TEM Imaging, EDX Elemental Mapping, and XAS Analysis. Electron microscopy and spectroscopic analysis were undertaken on parallel samples labeled with much higher

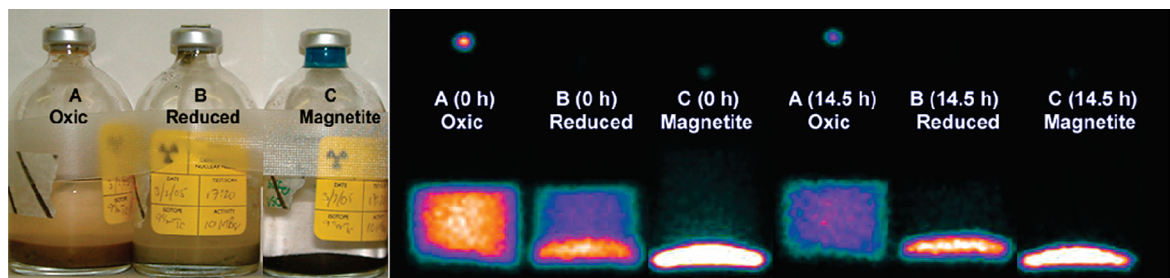


FIGURE 1. Start and end point γ -camera images for microcosm experiments. (A) Sediment oxic control; (B) sediment reduced sample; (C) magnetite (reducing control). Images were taken of samples approximately 5 min after injection of 0.1 mL of water containing ca. 10 MBq ^{99m}Tc (0 h) or following 14.5 h incubation.

^{99m}Tc concentrations to compliment the γ -camera imaging data, and to probe the fate of technetium within reduced sediments at a molecular scale. FRC sediments (1 g wet weight) from Area 2 were prereduced in batch experiments in the presence of 2 mL of basal freshwater medium containing 20 mM acetate. After 1 month of incubation at room temperature, $101 \pm 4\%$ of the sediment bound Fe was present as acid extractable Fe(II) as determined by ferrozine analyses (26, 27). Approximately 20 mg of prereduced FRC sediment in 50 μL of basal freshwater medium was then transferred under anaerobic conditions, reacted with 60 kBq (15 μM) ammonium pertechnetate, and left for 2 weeks after which time ca. 25% of the Tc had been removed from solution. After reaction, TEM specimens were prepared by washing samples twice in deoxygenated ethanol to dehydrate them, resin embedding by washing twice more using 100% PR white resin T, and finally adding resin and curing the samples at 70 $^{\circ}\text{C}$ for 24 h. The Tc-containing sediment was thin-sectioned to a thickness of 70–100 nm using an ultramicrotome and then mounted onto a standard TEM support grid. Specimens were examined using a Philips CM200 field emission gun scanning TEM fitted with an ultrathin window energy dispersive X-ray detector (Oxford Instruments ISIS EDX) to determine the distribution of Tc and Fe in the sample. Tc L and Tc K peaks were used for data analysis. Though the K peak is definitive for Tc it only provided a weak signal; the L peak was stronger but showed a potential interference with the S peak. Analysis of the sediment samples showed no detectable S in the elemental scans, thus the maps prepared using both the Tc L and K peaks are representative of Tc-rich areas in the sample.

X-ray absorption spectroscopy (XAS) was used to investigate the redox state and coordination environment of Tc in the samples, which were prepared and analyzed using methods detailed in previous studies (7, 10). Briefly, ca. 1 g wet weight samples of FRC column sediments in 10 mL of basal freshwater medium were spiked with ca. 0.14 mM ^{99m}Tc (85 kBq) and incubated until ca. 99% of the Tc had been removed from solution as measured using scintillation counting. The samples were frozen until mounted for analysis in anoxic sediment holders, transported to the Daresbury Synchrotron Radiation Source, and analyzed using X-ray absorption near edge structure (XANES; 4–8 scans). Data analysis was identical to that described in previous work (10, 36, 37).

Error Analysis. Unless otherwise noted, samples were analyzed in triplicate; error shown is standard error.

Results and Discussion

Visualization of ^{99m}Tc –Sediment Interactions in Batch Experiments. To determine if a ^{99m}Tc tracer solution could be used to image interactions between the radionuclide and Fe(II)-bearing mineral phases within the time-scales required for biogeochemical experiments, 10 MBq ^{99m}Tc was injected into sealed anoxic bottles to give a final concentration of 10

$\times 10^{-12}$ M ^{99m}Tc (Figure 1). The bottles contained slurries of oxidized and biologically reduced sediment from the US DoE Oak Ridge FRC site (Figure 1A and B), or a control Fe(II)-bearing mineral phase (biogenic magnetite, Figure 1C), known to reduce and precipitate Tc abiotically (38, 39). The biologically reduced sediment (10 g of sediment in 50 mL of suspension) was prepared by the addition of 10 mM acetate as an electron donor (as described previously (10)) and contained 50 mmol Fe(II) kg^{-1} sediment slurry (measured using the ferrozine assay; 26, 27). The biogenic magnetite was prepared by reduction of synthetic poorly crystalline ferric oxide by *Geobacter sulfurreducens* (24, 25) and contained approximately 30 mmol Fe(II) kg^{-1} mineral slurry. The ^{99m}Tc added to the magnetite sample was removed from solution quickly and concentrated with the mineral phase, which collected at the bottom of the bottle rapidly, and was clearly visible in the first γ -camera image (Figure 1C). Approximately 85% of the ^{99m}Tc was associated with the magnetite within only 5 min incubation and ca. 95% ^{99m}Tc was removed by 14.5 h. This was consistent with the expected rapid and efficient reduction of Tc(VII) by magnetite, to form Tc(IV) which likely sorbs to the magnetite at this low concentration. Similarly, ^{99m}Tc was concentrated in the solid phase of the prereduced FRC sediment, though not as rapidly or to the same extent (Figure 1B). This suggested that sediment bound Fe(II) could also reduce and immobilize ^{99m}Tc (VII) at picomolar concentrations over a 14 h time scale. In the bio-reduced FRC sediments, approximately 56% of the ^{99m}Tc was removed by the sediment in the first few minutes of the experiment with 90% removal after 14.5 h. In contrast, the ^{99m}Tc remained evenly distributed throughout the aqueous and sediment phases of an oxic FRC sediment slurry control, which contained no significant Fe(II) (Figure 1A).

Visualization of ^{99m}Tc Migration in Heterogeneous Sediment Columns. Visual inspection of sediment columns incubated with basal freshwater medium containing 50 mM acetate for 6 weeks showed the development of a redox gradient. A reddy brown colored, ferruginous oxic zone (ca. 1.5 cm deep) was present at the top of the sediment columns, and a gray–green zone formed below this suggesting active Fe(III) reduction was occurring ((40); Figure 2A). Channels from gas (for example CO_2 or N_2) produced during incubation were observed in acetate-enriched columns.

Following the addition of an aliquot of ^{99m}Tc (25 MBq) pumped through the columns at a rate of 7 mL hr^{-1} , γ -camera images showed a rapid passage of technetium through the oxic zone and retention of activity in the reduced zone (Figure 2B and C). Technetium was retained in the reduced zone even after 47 pore volumes of water had flushed through the column. Within 4 h, a hotspot of ^{99m}Tc activity was observed directly at the interface of the oxic and reduced sediment zones of the columns and it extended downward along channels in the sediment. By the end of the experiment (14.5 h), ca. 86% of the original ^{99m}Tc was retained within the

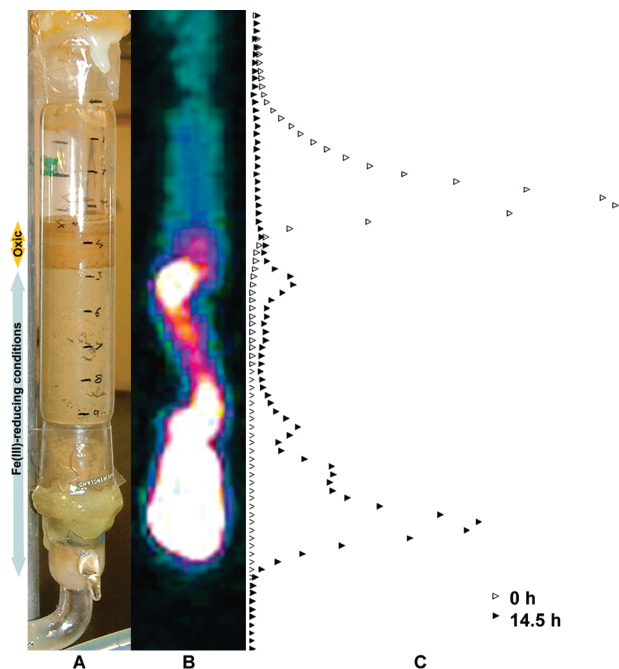


FIGURE 2. Summary of column experiment results. (A) Image of column incubated with 50 mM acetate (note zonation with column depth); (B) γ -camera image of column at 14.5 h (^{99m}Tc counts concentrated in white zones, decreasing through red, blue, and green areas); (C) decay corrected counts of ^{99m}Tc with depth in the sediment column for 0 h (open triangles) and 14.5 h (closed triangles) after injection with 0.5 mL of water containing 25 MBq ^{99m}Tc into the liquid headspace.

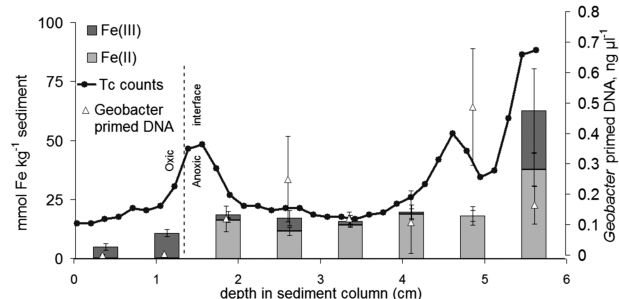


FIGURE 3. Bar chart showing the distribution of acid extractable Fe(II) and Fe(III) (mmol Fe kg^{-1} sediment). Line graph represents the relative abundance of ^{99m}Tc -associated activity. Scatter plot is the concentration of *Geobacter* primed DNA ($\text{ng } \mu\text{L}^{-1}$) with depth from the sediment surface.

reduced zones of the sediment columns (Figure 2). The other ca. 14% of the ^{99m}Tc spike was accounted for in the effluents.

Mineralogical, Geochemical and Microbiological Analyses of Columns. At the end of the experiment (14.5 h), the sediment columns were sectioned and analyzed across the redox boundary between depths of 1 and 6 cm where technetium accumulation occurred. This was to identify the biogeochemical controls underpinning localized concentrations of ^{99m}Tc within the sediment. The pH in column discs was circumneutral, and geochemical analyses of Fe speciation using the ferrozine assay (26, 41) found no extractable Fe(II) detectable in the oxic sediment zones. Higher concentrations of up to $38 \pm 7 \text{ mmol kg}^{-1}$ Fe(II) were observed deeper in the 50 mM acetate enriched column (Figure 3). High Tc counts were significantly correlated with elevated Fe(II) concentrations ($R^2 = 0.76$; $n = 8$). Interestingly, in a parallel column experiment conducted under similar flow conditions but with less acetate (10 mM), Fe(III) reduction was only partially stimulated, with only 16 ± 2

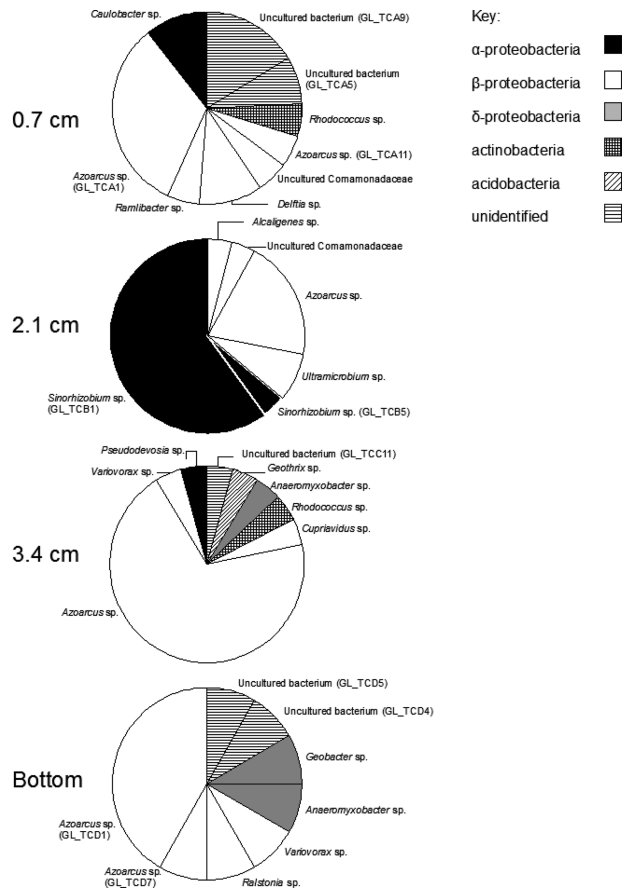


FIGURE 4. Composition of bacterial communities isolated from column incubated with 50 mM acetate, determined by 16S rRNA gene clone libraries. Clone libraries were constructed from sediment taken at 0.7, 2.1, and 3.4 cm below the column sediment surface and from the bottom of the column. Clone names (bracketed) are provided where two or more OTUs in a clone library belong to the same genus (for more detailed information, refer to Table SI-1).

mmol kg^{-1} Fe(II) measured at depth. In this partially reduced sediment column technetium retention was only ca. 39% compared to ca. 86% in the more reduced system. In the 50 mM acetate column, the concentrations of total extractable Fe (Fe(III) + Fe(II)) also increased with sediment depth (Figure 3), possibly a consequence of Fe-rich particles being transported down the core over time. Furthermore, Tc accumulated along the channels produced by gas genesis during column incubation, suggesting that in field conditions with similar channeled flow, there is still potential for immobilization of Tc providing that the sediments are Fe(III)-reducing.

Changes in the composition and structure of the microbial communities in the acetate-amended columns were examined to determine which organisms might be driving the geochemical processes leading to reduction and immobilization of Tc (Figure 4, Table SI-1). Analyses using broad specificity primers for bacterial 16S rRNA genes suggested that α - and β -proteobacteria dominated, including relatives of the known nitrate-reducing bacterium *Azoarcus* sp. HA (Clone GL TCA1), which were abundant throughout the sediment column. The addition of acetate is known to stimulate the growth and activity of members of this genus under denitrifying conditions (42) and they are also capable of degrading a wide-range of aromatic compounds, including toluene (43), an organic cocontaminant in FRC sediments. Within the deeper, anoxic, Fe(II)-bearing zone of the sediment column (≥ 3.4 cm), close relatives of Fe(III)-reducing organ-

isms such as *Geothrix* sp., *Anaeromyxobacter* sp., and *Geobacter* sp. were detected, which have previously been identified in FRC sediments (10, 44, 45). Prior studies have shown the addition of acetate stimulates both the growth and activity of *Geobacter* (46), increasing their capability to immobilize technetium in sediments via both direct and indirect mechanisms (11). More recently, Marshall et al. (47) documented, for the first time, the (Fe(II)-mediated) reduction of pertechnetate by *Anaeromyxobacter* strain 2CP-C. This organism contains an assortment of genes encoding redox associated proteins, including *c*-type cytochromes (48), efficient reductases for both Fe(II) and Tc(VII) in a number of different bacteria (49, 50). Organisms closely related to this strain (clone GL_TCD8 shares 98.8% sequence similarity, across 735 bp) were only detected within the Fe(II)-bearing zone of the sediment. To correlate the abundance of putative Fe(III)-reducing bacteria with Fe(II) concentrations and ^{99m}Tc activity in the sediment columns, we used qPCR to target members of the family *Geobacteraceae*, a commonly studied group of organisms associated with metal cycling in freshwater environments, and in particular the reduction of Fe(III) to Fe(II). This confirmed the increased abundance of *Geobacter*-primed DNA in the deeper sediment zones. Concentrations of *Geobacter* primed DNA were very low in the upper, oxic portion of the sediment column (Figure 3). Within the zone nearest to the sediment surface (i.e., ≤ 2.1 cm), 98% of the Operational Taxonomic Units (OTUs) detected with these *Geobacteraceae* targeted primers were most closely related to a *Pelobacter* species (clone GL TCGE01; see Table SI-2), which lacks the abundant *c*-type cytochromes found in other *Geobacteraceae* (51). This organism also comprised a significant proportion of the OTUs deeper in the sediment column, up to 35% of clones at depths ≥ 3.4 cm. However, with increasing depth, the proportion of close relatives of *Geobacter* sp. increased. These organisms comprised 54% of OTUs at 3.4 cm depth and 65% of OTUs at the bottom of the sediment column, and included close relatives of *G. metallireducens*, *G. humireducens*, and *G. chapellii*. The increased abundance of *Geobacteraceae* in parts of the column that had elevated Fe(II) concentrations and ^{99m}Tc activity further highlights the potential importance of members of this family in controlling the mobility of Tc within sediments contaminated with the radionuclide.

TEM and XAS analyses. To probe the fate of Tc within FRC sediments driven to Fe(III)-reducing conditions by the addition of 20 mM acetate, microcosms in parallel experiments were challenged with higher concentrations of ^{99m}Tc (VII) to allow direct spectroscopic analysis. Samples analyzed using transmission electron microscopy (TEM) with an energy dispersive X-ray detector showed an association of Tc with Fe-bearing mineral phases (Figure 5). Similar studies using electron energy-loss spectrometry (EELS) with Tc-spiked, Fe(III)-reducing estuarine sediments, also showed association of Tc with Fe(II), although we were unable to speciate the Fe in these FRC samples using this technique (unpublished data). However, X-ray absorption spectroscopy (XAS) analyses did allow us to determine the oxidation state of the immobilized technetium in the FRC sediments. Here, almost all (99%) of the Tc was removed from solution, and XANES analyses showed the sediment bound technetium was predominantly present as Tc(IV) (Figure SI-1), consistent with previous results (10, 37). It is important to note that the Tc concentration in the samples analyzed by TEM and XAS was up to 8 orders of magnitude greater than that used in the tracer column study, confirming that sediments that have undergone biogenic Fe(III)-reduction are capable of reducing technetium mobility over a broad range of concentrations.

Implications for the Application of γ -Camera Imaging. Despite their obvious potential for noninvasive monitoring at very low concentrations, nuclear imaging techniques have

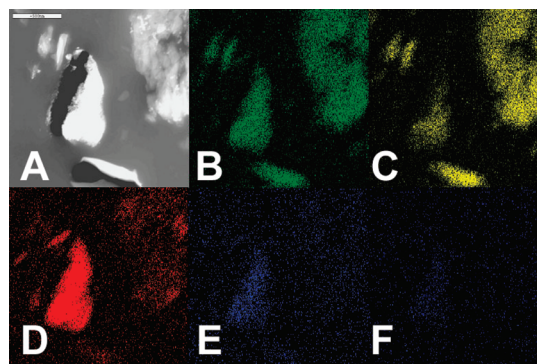


FIGURE 5. TEM and elemental imaging maps for a representative sample of Area 2 sediments incubated with ammonium pertechnetate (^{99m}Tc). (A) Darkfield image; (B–F) STEM maps of elemental distributions: B, aluminum; C, silicon; D, iron; E, Tc (L peak); and F, Tc (K peak). Scale bar in A is ca. 500 nm.

not been used to address the biogeochemical behavior of priority radionuclide contaminants. This study has demonstrated the potential for this technique to provide real time information on the mobility of technetium. When used in combination with geochemical, mineralogical, and microbiological techniques, γ -camera imaging of the fate of Tc(VII) has helped confirm that the biostimulation of Fe(III)-reducing bacteria is an effective mechanism for immobilizing the radionuclide in sediments, presumably by reduction to Tc(IV) over a broad concentration range. The precise mechanism of the rapid and efficient Tc immobilization noted in these column experiments at ultratrace concentrations is unclear, since a number of mechanisms could be operating simultaneously within the heterogeneous microenvironments present. Anaerobic bacteria, including Fe(III)-reducers have the potential to reduce Tc(VII) by enzymatic mechanisms (11, 13, 14), or abiotically via biogenic Fe(II) (3, 8, 11). Indeed, a variety of Fe(II)-containing minerals, including Fe(OH)₂, chlorite, siderite, and magnetite, are known to reduce Tc(VII) very efficiently (8, 11, 37, 39, 52, 53). On balance, an indirect mechanism mediated via biogenic Fe(II) is likely in our experiments given the rapid removal (<5 min) of ^{99m}Tc into the layers of prerduced sediment where ferrous iron had accumulated. In addition to the localization of Tc and Fe(II) within the column experiments, the concentrations of radionuclide used were far below those thought to be recognized efficiently by hydrogenases (54) or other enzymatic systems. Finally, it is worth noting that the isotope used for imaging (^{99m}Tc (VII)) is used as a conservative tracer in hydrological studies (18–22, 55). Given the very strong interactions of ^{99m}Tc (VII) with Fe(II), results from such studies should be interpreted with care, especially if they involve subsurface zones where Fe(II) may be present.

In addition to monitoring the transport and behavior of Tc in real time, there are many other potential applications of γ -camera imaging in biogeochemical studies. The relatively short half-life of ^{99m}Tc (6 h) reduces the risk of human and environmental exposure to harmful levels of radiation, while when properly handled, high-energy γ radiation enables detection of the radionuclides at ultratrace concentrations. Other γ -emitting radionuclides that could be imaged as geochemical analogues for environmentally relevant pollutants include mercury (^{203}Hg or possibly ^{197}Hg), chromium (^{51}Cr), cobalt (^{57}Co), and iodine (^{123}I). Positron-emitting radionuclides that potentially may be imaged but require a much more expensive positron emission tomography (PET) scanner to detect them include copper (^{64}Cu) and fluorine (^{18}F). Additionally, compounds labeled with radioisotopes such as ^{99m}Tc or ^{123}I could be used to examine the environmental behavior of many organic pollutants. In summary, the combination of approaches afforded by γ -camera imaging

of the type described here are currently underused but offer a potentially valuable, noninvasive tool for imaging ultratrace pollutant mobility in sediments and, in combination with geomicrobiological techniques, provides a unique insight into the behavior of technetium in the environment.

Acknowledgments

This research was supported by the U.S. DoE Office of Science, Office of Biological and Environmental Research, ERSD, Grant DE-FG02-04ER63743; NERC grant NE/D005361/1 and NE/D00473X/1; CCLRC Daresbury SRS Beamtime Award 46140; Universities UK Overseas Research Studentship; the University of Manchester; Bob Bilsborrow (Daresbury SRS), Dave Watson and Barry Kinsall (FRC sampling), staff at Manchester Royal Infirmary Department of Nuclear Medicine, and Miranda Keith-Roach for helpful manuscript comment. G.L. and J.M.M. contributed equally to this work.

Supporting Information Available

Figure SI-1 (XANES results), Tables SI-1 and SI-2 (phylogenetic affiliation of OTUs detected using 16S rRNA gene clone libraries), Table SI-3 (summary of sequencing primers used for PCR reactions in this study), and Table SI-4 (Fe(II) and Fe(tot) concentration data for column experiment). This material is available free of charge via the Internet at <http://pubs.acs.org>.

Literature Cited

- Morris, K.; Butterworth, J. C.; Livens, F. R. Evidence for the remobilization of Sellafield waste radionuclides in an intertidal salt marsh, West Cumbria, U.K. *Estuarine Coastal Shelf Sci.* **2000**, *51*, 613–625.
- Macaskie, L. The application of biotechnology to the treatment of wastes produced from the nuclear fuel cycle: biodegradation and bioaccumulation as a means of treating radionuclide-containing streams. *Crit. Rev. Biotechnol.* **1991**, *11*, 41–112.
- Wildung, R. E.; Li, S. W.; Murray, C. J.; Krupka, K. M.; Xie, Y.; Hess, N. J.; Roden, E. E. Technetium reduction in sediments of a shallow aquifer exhibiting dissimilatory iron reduction potential. *FEMS Microbiol. Ecol.* **2004**, *49*, 151–162.
- Lieser, K. H. Technetium in the nuclear-fuel cycle, in medicine and in the environment. *Radiochim. Acta* **1993**, *63*, 5–8.
- Champ, M. A.; Makeyev, V. V.; Brooks, J. M.; Delaca, T. E.; van der Horst, K. M.; Engle, M. V. Assessment of the impact of nuclear wastes in the Russian Arctic. *Mar. Pollut. Bull.* **1998**, *35*, 203–221.
- Burke, I. T.; Boothman, C.; Lloyd, J. R.; Livens, F. R.; Charnock, J. M.; McBeth, J. M.; Mortimer, R. J. G.; Morris, K. Reoxidation behavior of technetium, iron, and sulfur in estuarine sediments. *Environ. Sci. Technol.* **2006**, *40*, 3529–3535.
- Burke, I. T.; Boothman, C.; Lloyd, J. R.; Mortimer, R. J. G.; Livens, F. R.; Morris, K. Effects of progressive anoxia on the solubility of technetium in sediments. *Environ. Sci. Technol.* **2005**, *39*, 4109–4116.
- Fredrickson, J. K.; Zachara, J. M.; Kennedy, D. W.; Kukkadapu, R. K.; McKinley, J. P.; Heald, S. M.; Liu, C.; Plymale, A. E. Reduction of TcO_4^- by sediment-associated biogenic Fe(II). *Geochim. Cosmochim. Acta* **2004**, *68*, 3171–3187.
- Keith-Roach, M. J.; Morris, K.; Dahlgard, H. An investigation into technetium binding in sediments. *Mar. Chem.* **2003**, *81*, 149–162.
- McBeth, J. M.; Lear, G.; Morris, K.; Burke, I. T.; Livens, F. R.; Lloyd, J. R. Technetium reduction and reoxidation in aquifer sediments. *Geomicrobiol. J.* **2007**, *24*, 189–197.
- Lloyd, J. R.; Sole, V. A.; Van Praagh, C. V. G.; Lovley, D. R. Direct and Fe(II)-mediated reduction of technetium by Fe(III)-reducing bacteria. *Appl. Environ. Microbiol.* **2000**, *66*, 3743–3749.
- Lloyd, J. R.; Nolting, H.-F.; Solé, V. A.; Bosecker, K.; Macaskie, L. E. Technetium reduction and precipitation by sulfate-reducing bacteria. *Geomicrobiol. J.* **1998**, *15*, 45–58.
- Lloyd, J. R.; Cole, J. A.; Macaskie, L. E. Reduction and removal of heptavalent technetium from solution by *Escherichia coli*. *J. Bacteriol.* **1997**, *179*, 2014–2021.
- Lloyd, J. R.; Ridley, J.; Khizniak, T.; Lyalikova, N. N.; Macaskie, L. E. Reduction of technetium by *Desulfovibrio desulfuricans*: biocatalyst characterization and use in a flowthrough bioreactor. *Appl. Environ. Microbiol.* **1999**, *65*, 2691–2696.

- Abdelouas, A.; Fattahi, M.; Grambow, B.; Vichot, L.; Gautier, E. Precipitation of technetium by subsurface sulfate-reducing bacteria. *Radiochim. Acta* **2002**, *90*, 773–777.
- Lloyd, J. R.; Renshaw, J. C. Bioremediation of radioactive waste: radionuclide-microbe interactions in laboratory and field-scale studies. *Curr. Opin. Biotechnol.* **2005**, *16*, 254–260.
- Richards, P.; Tucker, W. D.; Srivastava, S. C. Technetium-99m: An historical perspective. *Int. J. Appl. Radiat. Isot.* **1982**, *33*, 793–799.
- Hughes, C. E.; Airey, P. L.; Duran, E. B.; Miller, B. M.; Sombrito, E. Using radiotracer techniques for coastal hydrodynamic model evaluation. *J. Environ. Radioactiv.* **2004**, *76*, 195–206.
- Widestrand, H.; Andersson, P.; Byegård, J.; Skarnemark, G.; Skållberg, M.; Wass, E. In Situ Migration Experiments at Aspö Hard Rock Laboratory, Sweden: Results of Radioactive Tracer Migration Studies in a Single Fracture. *J. Radioanal. Nucl. Chem.* **2001**, *250*, 501–517.
- Perret, J.; Prasher, S. O.; Kantzas, A.; Hamilton, K.; Langford, C. Preferential Solute Flow in Intact Soil Columns Measured by SPECT Scanning. *Soil Sci. Soc. Am. J.* **2000**, *64*, 469–477.
- Jurisson, S.; Landa, E. R. Sorption of Tc-99m radiopharmaceutical compounds by soils. *Health Phys.* **2004**, *87*, 423–428.
- Borroto, J. I.; Dominguez, J.; Griffith, J.; Fick, M.; Leclerc, J. P. Technetium-99m as a tracer for the liquid RTD measurement in opaque anaerobic digester: application in a sugar wastewater treatment plant. *Chem. Eng. Process.* **2003**, *42*, 857–865.
- Caccavo, F., Jr.; Lonergan, D. J.; Lovley, D. R.; Davis, M.; Stolz, J. F.; McInerney, M. J. *Geobacter sulfurreducens* sp. nov., a hydrogen and acetate-oxidizing dissimilatory metal reducing microorganism. *Appl. Environ. Microbiol.* **1994**, *60*, 3752–3759.
- Lovley, D. R.; Fraga, J. L.; Coates, J. D.; Blunt-Harris, E. L. Humics as an electron donor for anaerobic respiration. *Environ. Microbiol.* **1999**, *1*, 89–98.
- Lovley, D. R.; Phillips, E. J. P. Novel mode of microbial energy metabolism: organic carbon oxidation coupled to dissimilatory reduction of iron or manganese. *Appl. Environ. Microbiol.* **1988**, *54*, 1472–1480.
- Stookey, L. L. Ferrozine - a new spectrophotometric reagent for iron. *Anal. Chem.* **1970**, *42*, 779–781.
- Lovley, D. R.; Phillips, E. J. P. Availability of ferric iron for microbial reduction in bottom sediments of the freshwater tidal Potomac River. *Appl. Environ. Microbiol.* **1986**, *52*, 751–757.
- Eden, P.; Schmidt, T.; Blakemore, R.; Pace, N. Phylogenetic analysis of *Aquaspirillum magnetotacticum* using polymerase chain reaction-amplified 16S rRNA-specific DNA. *Int. J. Syst. Bacteriol.* **1991**, *41*, 324–325.
- Weisburg, W. G.; Barns, S. M.; Pelletier, D. A.; Lane, D. J. 16S ribosomal DNA amplification for phylogenetic study. *J. Bacteriol.* **1991**, *173*, 697–703.
- Lane, D. J.; Pace, B.; Olsen, G. J.; Stahl, D. A.; Sogin, M. L.; Pace, N. R. Rapid determination of 16S ribosomal RNA sequences for phylogenetic analyses. *Proc. Natl. Acad. Sci. U.S.A.* **1985**, *82*, 6955–6959.
- Lane, D. J. 16S/23S rRNA sequencing. In *Nucleic Acid Techniques in Bacterial Systematics*; Stackebrandt, E.; Goodfellow, M., Eds. John Wiley & Sons: New York, 1991; pp 115–175.
- Giovannoni, S. J.; DeLong, E. F.; Olsen, G. J.; Pace, N. R. Phylogenetic group-specific oligodeoxynucleotide probes for identification of single microbial cells. *J. Bacteriol.* **1988**, *170*, 720–726.
- Holmes, D. E.; Finneran, K. T.; O'Neil, R. A.; Lovley, D. R. Enrichment of members of the family Geobacteraceae associated with stimulation of dissimilatory metal reduction in uranium-contaminated aquifer sediments. *Appl. Environ. Microbiol.* **2002**, *68*, 2300–2306.
- Anderson, R. T.; Rooney-Varga, J. N.; Gaw, C. V.; Lovley, D. R. Anaerobic benzene oxidation in the Fe(III) reduction zone of petroleum-contaminated aquifers. *Environ. Sci. Technol.* **1998**, *32*, 1222–1229.
- Altschul, S. F.; Gish, W.; Miller, W.; Myers, E. W.; Lipman, D. J. Basic local alignment search tool. *J. Mol. Biol.* **1990**, *215*, 403–410.
- Morris, K.; Livens, F. R.; Charnock, J. M.; Burke, I. T.; McBeth, J. M.; Boothman, C.; Lloyd, J. R. Microbially Driven Transformations of Technetium. In Proceedings of the 4th workshop on speciation, techniques, and facilities for radioactive materials at synchrotron light sources, Karlsruhe, Germany, 18–20 Sept 2006; Nuclear Energy Agency: Karlsruhe, Germany, 2007; pp 71–81.

- (37) Morris, K.; Livens, F. R.; Charnock, J. M.; Burke, I. T.; McBeth, J. M.; Begg, J. D. C.; Boothman, C.; Lloyd, J. R. An X-ray absorption study of the fate of technetium in reduced and reoxidised sediments and mineral phases. *Appl. Geochem.* **2008**, *23*, 603–617.
- (38) Maes, A.; Geraedts, K.; Bruggeman, C.; VanCluysen, J.; Rossberg, A.; Hennig, C. Evidence for the interaction of technetium colloids with humic substances by X-ray absorption spectroscopy. *Environ. Sci. Technol.* **2004**, *38*, 2044–2051.
- (39) Cui, D. Q.; Eriksen, T. E. Reduction of pertechnetate in solution by heterogeneous electron transfer from Fe(II)-containing geological material. *Environ. Sci. Technol.* **1996**, *30*, 2263–2269.
- (40) Lovley, D. R. Dissimilatory Fe(III) and Mn(IV) reduction. *Microbiol. Rev.* **1991**, *55*, 259–287.
- (41) Lovley, D. R.; Phillips, E. J. P. Rapid assay for microbially reducible ferric iron in aquatic sediments. *Appl. Environ. Microb.* **1987**, *53*, 1536–1540.
- (42) Reinhold-Hurek, B.; Hurek, T. The Genera *Azoarcus*, *Azovibrio*, *Azospira* and *Azonexus*. In *The Prokaryotes*, 3rd ed.; Dworkin, M., Ed.; Springer: Singapore, 2006; Vol. 5 (Proteobacteria: Alpha and Beta Subclasses); pp 873–891.
- (43) Zhou, J.; Fries, M. R.; Chee-Sanford, J. C.; Tiedje, J. M. Phylogenetic analyses of a new group of denitrifiers capable of anaerobic growth of toluene and description of *Azoarcus toluyliticus* sp. nov. *Int. J. Syst. Bacteriol.* **1995**, *45*, 500–506.
- (44) Shelobolina, E. S.; O'Neill, K. R.; Finneran, K. T.; Hayes, L. A.; Lovley, D. R. Potential for *in-situ* bioremediation of a low-pH, high-nitrate uranium-contaminated groundwater. *Soil Sediment Contam.* **2003**, *12*, 865–884.
- (45) North, N. N.; Dollhopf, S. L.; Petrie, L.; Istok, J. D.; Balkwill, D. L.; Kostka, J. E. Change in bacterial community structure during in situ biostimulation of subsurface sediment cocontaminated with uranium and nitrate. *Appl. Environ. Microbiol.* **2004**, *70*, 4911–4920.
- (46) Holmes, D. E.; O'Neil, R. A.; Vrionis, H. A.; N'Guessan, L. A.; Ortiz-Bernad, I.; Larrahondo, M. J.; Adams, L. A.; Ward, J. A.; Nicoll, J. S.; Nevin, K. P.; Chavan, M. A.; Johnson, J. P.; Long, P. E.; Lovley, D. R. Subsurface clade of *Geobacteraceae* that predominates in a diversity of Fe(III)-reducing subsurface environments. *ISME J.* **2007**, *1*, 663–677.
- (47) Marshall, M. J.; Dohnalkova, A. C.; Kennedy, D. W.; Plymale, A. E.; Thomas, S. H.; Löffler, F. E.; Sanford, R. A.; Zachara, J. M.; Fredrickson, J. K.; Beliaev, A. S. Electron donor-dependent radionuclide reduction and nanoparticle formation by *Anaeromyxobacter dehalogenans* strain 2CP-C. *Environ. Microbiol.* **2009**, *11*, 534–543.
- (48) Thomas, S. H.; Wagner, R. D.; Arakaki, A. K.; Skolnick, J.; Kirby, J. R.; Shimkets, L. J.; Sanford, R. A.; Löffler, F. E. The Mosaic Genome of *Anaeromyxobacter dehalogenans* Strain 2CP-C Suggests an Aerobic Common Ancestor to the Delta-Proteobacteria. *PLoS ONE* **2008**, *3*, e2103.
- (49) Marshall, M. J.; Plymale, A. E.; Kennedy, D. W.; Shi, L.; Wang, Z.; Reed, S. B.; Dohnalkova, A. C.; Simonson, C. J.; Liu, C.; Saffarini, D. A.; Romine, M. F.; Zachara, J. M.; Beliaev, A. S.; Fredrickson, J. K. Hydrogenase- and outer membrane c-type cytochrome-facilitated reduction of technetium(VII) by *Shewanella oneidensis* MR-1. *Environ. Microbiol.* **2008**, *10*, 125–136.
- (50) Seeliger, S.; Cord-Ruwisch, R.; Schink, B. A Periplasmic and Extracellular c-Type Cytochrome of *Geobacter sulfurreducens* Acts as a Ferric Iron Reductase and as an Electron Carrier to Other Acceptors or to Partner Bacteria. *J. Bacteriol.* **1998**, *180*, 3686–3691.
- (51) Haveman, S. A.; Holmes, D. E.; Ding, Y.-H. R.; Ward, J. E.; DiDonato, R. J., Jr.; Lovley, D. R. c-Type Cytochromes in *Pelobacter carbinolicus*. *Appl. Environ. Microbiol.* **2006**, *72*, 6980–6985.
- (52) Vandergraaf, T. T.; Ticknor, K. V.; George, I. M. Reactions between technetium in solution and iron-containing minerals under oxic and anoxic conditions. In *Geochemical Behavior of Disposed Radioactive Waste*; Barney, G. S., Navratil, J. D., Schulz, W. W., Eds.; American Chemical Society: Washington, DC, 1984; Vol 246, pp 25–43.
- (53) Cui, D. Q.; Eriksen, T. E. Reduction of pertechnetate by ferrous iron in solution: Influence of sorbed and precipitated Fe(II). *Environ. Sci. Technol.* **1996**, *30*, 2259–2262.
- (54) Lloyd, J. R.; Harding, C. L.; Macaskie, L. E. Tc(VII) reduction and accumulation by immobilized cells of *Escherichia coli*. *Bio-technol. Bioeng.* **1997**, *55*, 505–510.
- (55) Aarkrog, A.; Chen, Q.; Dahlgaard, H.; Nielsen, S. P.; Trapeznikov, A.; Pozolotina, V. Evidence of ⁹⁹Tc in Ural river sediments. *J. Environ. Radioactiv.* **1997**, *37*, 201–213.

ES802885R